CrossMark

RESEARCH PAPER

LC-high resolution-MS/MS for identification of 69 metabolites of the new psychoactive substance 1-(4-ethylphenyl-)-N-[(2-methoxyphenyl)methyl] propane-2-amine (4-EA-NBOMe) in rat urine and human liver S9 incubates and comparison of its screening power with further MS techniques

Achim T. Caspar[1] · Folker Westphal[2] · Markus R. Meyer[1] · Hans H. Maurer[1]

Abstract 4-EA-NBOMe (N-(2-methoxybenzyl)-4-ethylamphetamine, 1-(4-ethylphenyl-)-N-[(2-methoxyphenyl)methyl]propane-2-amine) is an amphetamine-derived new psychoactive substance (NPS) of the N-methoxybenzyl (NBOMe) group first seized by German custom authorities. In contrast to the phenethylamine NBOMes, studies on the pharmacological, toxicological, or metabolic properties are not yet published. The aims of the presented work were the use of LC-HR-MS/MS for identification of the phase I and II metabolites of 4-EA-NBOMe in rat urine and pooled human S9 fraction (pS9) incubations, to compare metabolite formation in both models, to identify involved monooxygenases, and to elucidate its detectability in standard urine screening approaches (SUSAs) using GC-MS, LC-MS^n, and LC-HR-MS/MS. 4-EA-NBOMe was mainly metabolized by oxidation of the ethyl group to phenyl acetaldehyde, to benzoic acid, or to phenylacetic acid, by hydroxylation, and all combined with O-demethylation as well as by glucuronidation and sulfation of the main phase I metabolites in rats. With the exception of the oxidation to benzoic acid, all main metabolic reactions could be confirmed in the incubations with pS9. In total, 36 phase I and 33 phase II metabolites could be identified. Monooxygenase activity screenings revealed the general involvement of cytochrome-P450 (CYP) 1A2, CYP2B6, and CYP3A4. An intake of 4-EA-NBOMe was detectable only via its metabolites by all SUSAs after low-dose administration. The main targets for both LC-MS screenings should be the phenylacetic acid derivative, the mandelic acid derivative both with and without additional O-demethylation, and, for GC-MS, the hydroxy metabolite after conjugate cleavage.

Keywords LC-HR-MS/MS · 4-EA-NBOMe · New psychoactive substance · Metabolism · pS9

Published in the topical collection celebrating *ABCs 16th Anniversary*.

✉ Hans H. Maurer
hans.maurer@uks.eu

[1] Department of Experimental and Clinical Toxicology, Institute of Experimental and Clinical Pharmacology and Toxicology, Saarland University, 66421 Homburg, Saarland, Germany

[2] Section Narcotics/Toxicology, State Bureau of Criminal Investigation Schleswig-Holstein, Mühlenweg 166, 24116 Kiel, Germany

Introduction

Among the new psychoactive substances (NPS), so-called N-2-methoxybenzyl derivatives (NBOMes) of phenethylamine-type drugs of abuse (2C derivatives) gained more and more importance in the last few years because of their widespread consumption and associated health risks [1–4]. Most studies have been published on pharmacological and metabolic properties of 2-(4-bromo-2,5-dimethoxyphenyl)-N-[(2-methoxyphenyl)methyl] ethanamine (25B-NBOMe), 2-(4-chloro-2,5-dimethoxyphenyl)-N-[(2-methoxyphenyl)methyl] ethanamine (25C-NBOMe), and 2-(4-iodo-2,5-dimethoxyphenyl)-N-[(2-methoxyphenyl)methyl] ethanamine (25I-NBOMe) [5–17]. Acute poisonings or even fatalities were described caused by wrong dosage or mislabeling of sold preparations (e.g., sold as 2C-B or LSD) [8, 9, 12, 13, 18–23]. Meanwhile, 25B-, 25C-, and 25I-NBOMe were scheduled in

Germany and many other countries with the consequence that new derivatives appeared. Recently, Westphal et al. [24] described the detection and the analytical behaviors of four amphetamine-type NBOMe derivatives first seized by the German custom authorities. Besides other NBOMe-type compounds, one of the crystalline substances could be identified as racemic 4-EA-NBOMe hydrochloride (*N*-(2-methoxybenzyl)4-ethylamphetamine; 1-(4-ethylphenyl-)*N*-[(2-methoxyphenyl)methyl]propane-2-amine), which is the NBOMe analogue of 4-ethylamphetamine (4-EA). To date, their pharmacological or pharmacokinetic properties have not been published. In case of the 2C derivatives, addition of the *N*-methoxybenzyl part increased the affinity to the serotonin receptor 5-HT$_{2A}$ significantly [25–28]. The amphetamine part could lead to stimulating effects as described for many amphetamine-like compounds [29]. However, in accordance to other NBOMe derivatives, it could be assumed that these amphetamine-type NBOMes have potent binding affinities to serotonergic, adrenergic, or dopaminergic receptors or transporters leading to hallucinogenic and/or stimulating effects. Although enantioselective differences in binding affinities or metabolism might be possible, they were not within the aims of the present work. The dosage should most probably be low according to high potency and very low dosages of 25B-, 25C-, and 25I-NBOMe applied as blotter papers or nose sprays [8, 9, 13, 18–20, 22, 30, 31]. Although such data for 4-EA-NBOMe are still missing, the aim of the present study was to use the power of LC-HR-MS/MS for identification of the in vivo and in vitro phase I and II metabolites of 4-EA-NBOMe in rat urine and pooled human S9 fraction (pS9) incubations, to compare metabolite formation in both models due to the lack of authentic human samples, and finally to elucidate its detectability in standard urine screening approaches (SUSAs) using GC-MS, LC-MS^n, and LC-HR-MS/MS, respectively. This should allow, as shown for many other newly emerging drugs in the past, to detect this new substance and/or its metabolites in clinical or forensic toxicology cases.

Experimental

Chemicals and reagents

Racemic 4-EA-NBOMe hydrochloride was provided by the State Bureau of Criminal Investigation Schleswig-Holstein (Kiel, Germany) for research purposes. Isocitrate, isocitrate dehydrogenase, superoxide dismutase, 3′-phosphoadenosine-5′-phosphosulfate (PAPS), *S*-(5′-adenosyl)-L-methionine (SAM), dithiothreitol (DTT), reduced glutathione (GSH), acetyl carnitine transferase (AcT), acetyl carnitine, acetyl coenzyme A (AcCoA), and carnitine were all purchased from

Sigma (Taufkirchen, Germany), NADP$^+$ from Biomol (Hamburg, Germany), and acetonitrile (LC-MS grade), ammonium formate (analytical grade), formic acid (LC-MS grade), methanol (LC-MS grade), and all other chemicals and reagents (analytical grade) from VWR (Darmstadt, Germany). Pooled human liver S9 fraction (pS9, 20 mg protein/mL, from 30 individual donors), UGT reaction mix solution A (25 mM UDP-glucuronic acid), UGT reaction mix solution B (250 mM Tris–HCl, 40 mM MgCl$_2$, and 0.125 mg/mL alamethicin), and baculovirus-infected insect cell microsomes (Supersomes) containing 1 nmol/mL of human complementary DNA-expressed cytochrome-P450 monooxygenases (CYP) 1A2, CYP2A6, CYP2B6, CYP2C8, CYP2C9, CYP2C19, CYP2D6, CYP2E1 (2 nmol/mL), CYP3A4, CYP3A5 (2 nmol/mL), or flavin-containing monooxygenase FMO3 (5 mg protein/mL) were obtained from Corning (Amsterdam, The Netherlands). After delivery, the enzyme preparations and CYPs were thawed at 37 °C, aliquoted, snap-frozen in liquid nitrogen, and stored at −80 °C until use.

Urine samples

According to established study designs [5, 6, 32], the investigations were performed using rat urine samples from male Wistar rats (Charles River, Sulzfeld, Germany) for toxicological diagnostic reasons according to German law. The compound was administered in an aqueous suspension by gastric intubation of a single dose each of 10 mg/kg body weight (BW) for identification of the metabolites and 0.1 mg/kg BW for estimation of the detectability after expected low-dose application. The rats were housed in metabolism cages for 24 h, having water ad libitum. Urine was collected separately from feces over a 24-h period. Blank urine samples were collected before drug administration to verify that the samples were free of interfering compounds. The samples were directly analyzed, aliquoted, and then stored at −20 °C.

Sample preparation for identification of phase I and II metabolites by LC-HR-MS/MS in rat urine

According to published procedures [32, 33], 100 μL of urine was mixed with 500 μL of acetonitrile for precipitation. After shaking and centrifugation, the supernatant was gently evaporated to dryness and reconstituted in 50 μL of a mixture of 10 mM aqueous ammonium formate buffer and acetonitrile (1:1, *v/v*) and 1 μL injected onto the LC-HR-MS/MS system with the conditions described below.

Incubation conditions for human in vitro metabolism studies

Incubation conditions for identification of phase I and II metabolites by LC-HR-MS/MS in pS9

The incubation conditions were in accordance to the experimental design developed by Richter et al. [34]. With a final protein concentration of 2 mg/mL, pS9 were pre-incubated for 10 min at 37 °C with 25 μg/mL alamethicin (UGT reaction mix solution B), 90 mM phosphate buffer (pH 7.4), 2.5 mM Mg^{2+}, 2.5 mM isocitrate, 0.6 mM $NADP^+$, 0.8 U/mL isocitrate dehydrogenase, 100 U/mL superoxide dismutase, 0.1 mM AcCoA, 2.3 mM acetyl carnitine, and 8 U/mL carnitine acetyltransferase. Thereafter, 2.5 mM UDP-glucuronic acid (UGT reaction mix solution A), 40 μM aqueous PAPS, 1.2 mM SAM, 1 mM DTT, 10 mM GSH, and 25 μM substrate in phosphate buffer were added to reach a final volume of the incubation mixture of 150 μL. All given concentrations are final concentrations. The reactions were started by addition of the substrate and the mixture was incubated for 60 and 480 min, respectively. A 60-μL aliquot of the mixture was transferred into a reaction tube after 60 min and the reactions were terminated with 20 μL ice-cold acetonitrile. The remaining mixture was incubated for additional 7 h and thereafter 30 μL ice-cold acetonitrile was added to stop the reaction. The solutions were cooled for 30 min at −18 °C, centrifuged for 2 min at 14,000 rpm, and the supernatants were transferred into an autosampler vial and 5 μL injected onto the LC-HR-MS/MS system with the conditions described below. Blank incubations without substrate and control samples without pS9 were prepared to confirm the absence of interfering compounds and to identify non-metabolically originated compounds.

Incubation conditions for monooxygenases (CYPs, FMO3) activity screening

According to standard procedures [6, 35, 36], microsomal incubations were performed at 37 °C at a concentration of 2.5 μM 4-EA-NBOMe, with the isozymes (50 pmol/mL, each) CYP1A2, CYP2A6, CYP2B6, CYP2C8, CYP2C9, CYP2C19, CYP2D6, CYP2E1, CYP3A4, CYP3A5, or FMO3 (0.25 mg protein/mL) for 30 min. Besides enzymes and substrates, the incubation mixtures (final volume, 50 μL) contained 90 mM phosphate buffer (pH 7.4), 5 mM Mg^{2+}, 5 mM isocitrate, 1.2 mM $NADP^+$, 0.5 U/mL isocitrate dehydrogenase, and 200 U/mL superoxide dismutase. For incubations with CYP2A6 and CYP2C9, phosphate buffer was replaced with 45 mM or 90 mM Tris buffer, respectively, according to the Gentest manual. Reactions were initiated by addition of the enzymes and stopped with 50 μL of ice-cold acetonitrile. The solution was centrifuged for 2 min at

14,000 rpm; 70 μL of the supernatant phase were transferred to an autosampler vial and 5 μL injected onto the LC-HR-MS/MS system.

LC-HR-MS/MS instrumentation for identification of phase I and II metabolites

According to published procedures [6, 34], the extracts were analyzed using a ThermoFisher Scientific (TF, Dreieich, Germany) Dionex UltiMate 3000 RS pump consisting of a degasser, a quaternary pump, and an UltiMate autosampler, coupled to a TF Q-Exactive Plus system equipped with a heated electrospray ionization (HESI)-II source. The instrument was operated in positive ionization mode. Mass calibration was performed prior to analysis according to the manufacturer's recommendations using external mass calibration.

Gradient elution was run on a TF Accucore PhenylHexyl column (100 mm × 2.1 mm, 2.6 μm) with column oven temperature of 60 °C. The mobile phases consisted of 2 mM aqueous ammonium formate containing formic acid (0.1%, v/v) and acetonitrile (1%, v/v, pH 3, eluent A) and 2 mM ammonium formate solution with acetonitrile/methanol (50:50, v/v) containing formic acid (0.1%, v/v) and water (1%, v/v, eluent B). First, the pH value of the aqueous solution was measured before addition of 1% acetonitrile. Second, for eluent B, ammonium formate was dissolved in methanol plus 1% water and then acetonitrile was added to the final volume. The gradient was programmed as follows: 0–1 min hold 98% A, 1–17 min 98% A to 2% A, 17–18 min hold 2% A, and 18–20 min hold 98% A, constantly at a flow rate of 500 μL/min.

The HESI-II source conditions were as follows: sheath gas, 60 arbitrary units (AU); auxiliary gas, 10 AU; spray voltage, 3.00 kV; heater temperature, 320 °C; ion transfer capillary temperature, 320 °C; and S-lens RF level, 60.0. Mass spectrometry was performed in positive polarity mode using full scan (FS) data and a subsequent data dependent acquisition (DDA) mode with inclusion lists containing the m/z values of expected phase I and II metabolites. Additionally, DDA runs without an inclusion list were performed to detect unexpected metabolites.

The settings for FS data acquisition were as follows: resolution, 35,000; microscans, 1; automatic gain control (AGC) target, 1e6; maximum injection time (IT), 120 ms; and scan range, m/z 100–700. The settings for the DDA mode with and without inclusion list were as follows: option with inclusion list "do not pick others," enabled; dynamic exclusion, 1.0 s; resolution, 17,500; microscans, 1; loop count, 5; AGC target, 2e5; maximum IT, 250 ms; isolation window, 1.0 m/z, high collision dissociation (HCD) with stepped normalized collision energy (NCE), 17.5, 35, and 52.5%; spectrum data type, profile; and underfill ratio, 0.5%. Xcalibur Qual Browser software version 2.2 SP1 was used for data handling.

For analyzing the in vitro incubations (monooxygenases and pS9), the MS settings and the mobile phases as well as the gradient and flow rate were the same with the same inclusion lists as for identification of metabolites.

Standard urine screening approaches

The SUSAs were performed as described in the following references: GC-MS SUSA [37, 38], LC-MS^n SUSA [5, 33], and LC-HR-MS/MS SUSA [5, 39].

Results and discussion

LC-HR-MS for identification of 4-EA-NBOMe and its phase I metabolites based on MS/MS fragmentation

In the following part, the HR-MS/MS fragmentation patterns of 4-EA-NBOMe and its metabolites (Fig. 1) will be discussed and exemplified for selected metabolites representing the general identification procedure. Due to the high number of the metabolites, not all were discussed in detail. A list of all detected phase I metabolites is given in Table S1 in the Electronic Supplementary Material (ESM). It contains the sample in which the compounds were detected, the precursor mass recorded in MS^1, the corresponding characteristic fragment ions in MS^2, the calculated exact masses, the corresponding elemental composition, the deviation of the measured from the calculated masses in ppm, and the retention times.

The HR-MS data indicated, according to previous published NBOMe metabolism studies [5–7], that the molecules could be broken down into two parts, the NBOMe part (fragment ion at m/z 121.0653, $C_8H_9O^+$, see Fig. 1), usually forming the most abundant fragment ions in the MS^2 spectra, and the amphetamine part (see Fig. 1). For spectra interpretation and identification of the expected metabolites based on the accurate precursor masses (PM) and calculated molecular formulas, the fragment ions of unmodified or modified NBOMe part were used (according to Fig. 1 and ESM Table S1). Metabolites formed by combinations of the described metabolic reactions were identified accordingly. As already described for other NBOMes [5, 6], the MS^2 spectra of the parent compounds and metabolites with unmodified NBOMe part showed only two abundant fragment ions formed by the NBOMe part (m/z 91.0548, $C_7H_7^+$ and m/z 121.0653, $C_8H_9O^+$), whereas the fragment ions coming from the phenethylamine parts showed very low abundances. But after O-demethylation of the NBOMe part, the fragment ions of the phenethylamine parts were more abundant besides the usually most abundant fragment ion of O-demethylated NBOMe part (m/z 107.0497, $C_7H_7O^+$) [5, 6]. Also, after N-demethoxybenzylation, the MS^2 spectra allowed better interpretation concerning the metabolic reactions at the

amphetamine core. Therefore, the general fragmentation patterns and spectra interpretation will be discussed here for N-demethoxybenzylated and O-demethylated metabolites according to Fig. 1. Spectra information received by the O-demethylated metabolites were used for interpretation of the spectra of metabolites without O-demethylation and confirmed by the measured accurate PM and the suggested molecular formulas. All PM are given with the calculated exact protonated masses. Numbering of the given compounds was in accordance to Table S1 (see ESM). Based on the described procedure, 36 phase I metabolites could be detected.

4-EA-NBOMe

4-EA-NBOMe (**1**, PM at m/z 284.2009, $C_{19}H_{26}ON^+$) showed a fragmentation pattern similar to most already described NBOMes and metabolites [5–7]. Cleavage of the N-C bond formed the most abundant and characteristic fragment ion at m/z 121.0653 ($C_8H_9O^+$) and a low-abundant (<1%, ESM Table S1) fragment ion at m/z 162.1283 ($C_{11}H_{16}N^+$). A loss of CH_2O (−30.0105 u) led to the tropylium ion at m/z 91.0548 ($C_7H_7^+$) also characteristic for other NBOMes. The low-abundant (<1%, ESM Table S1) fragment ion at m/z 147.1174 ($C_{11}H_{15}^+$) was formed by the loss of NH (−15.0109 u) from the iminium ion at m/z 162.1283 ($C_{11}H_{16}N^+$).

N-Demethoxybenzyl-phenyl acetaldehyde-4-EA-NBOMe

According to Fig. 1, the fragmentation pattern of the N-demethoxybenzyl-phenyl acetaldehyde metabolite (**3**, PM at m/z 178.1226, $C_{11}H_{16}ON^+$) showed, as expected, an initial loss of ammonia (−17.0260 u, NH_3) producing the fragment ion at m/z 161.0966 ($C_{11}H_{13}O^+$), followed by a loss of an ethylene group (−28.0313, C_2H_4) forming the most abundant fragment ion at m/z 133.0653 ($C_9H_9O^+$). A further loss of CO (−27.9949 u) produced the fragment ion at m/z 105.0704 ($C_8H_9^+$). The MS^2 spectrum of this metabolite was used for discussion of the position of the oxo group (+13.9792 u, +O, −2H). In the chemical structure of the N-demethoxybenzyl metabolite (**2**), four possible positions are available for introduction of an oxo group. The methyl group at the α-carbon next to the nitrogen could be oxidized but this reaction is not common and unlikely to happen. If oxidized at this position, an initial loss of formaldehyde would be expected and the fragment ion at m/z 133.0653 ($C_9H_9O^+$) could not be formed. The second possible position was the α-carbon next to the aromatic ring system. Oxidation of this position would lead to a cathinone-like structure. According to reference spectra [40, 41], most cathinones were characterized by an initial loss of water (−18.0106 u, H_2O) usually producing the most abundant fragment ion of the corresponding spectrum (even higher than an initial loss of ammonia). In any spectrum of the detected metabolites in this study, an initial loss of water was not
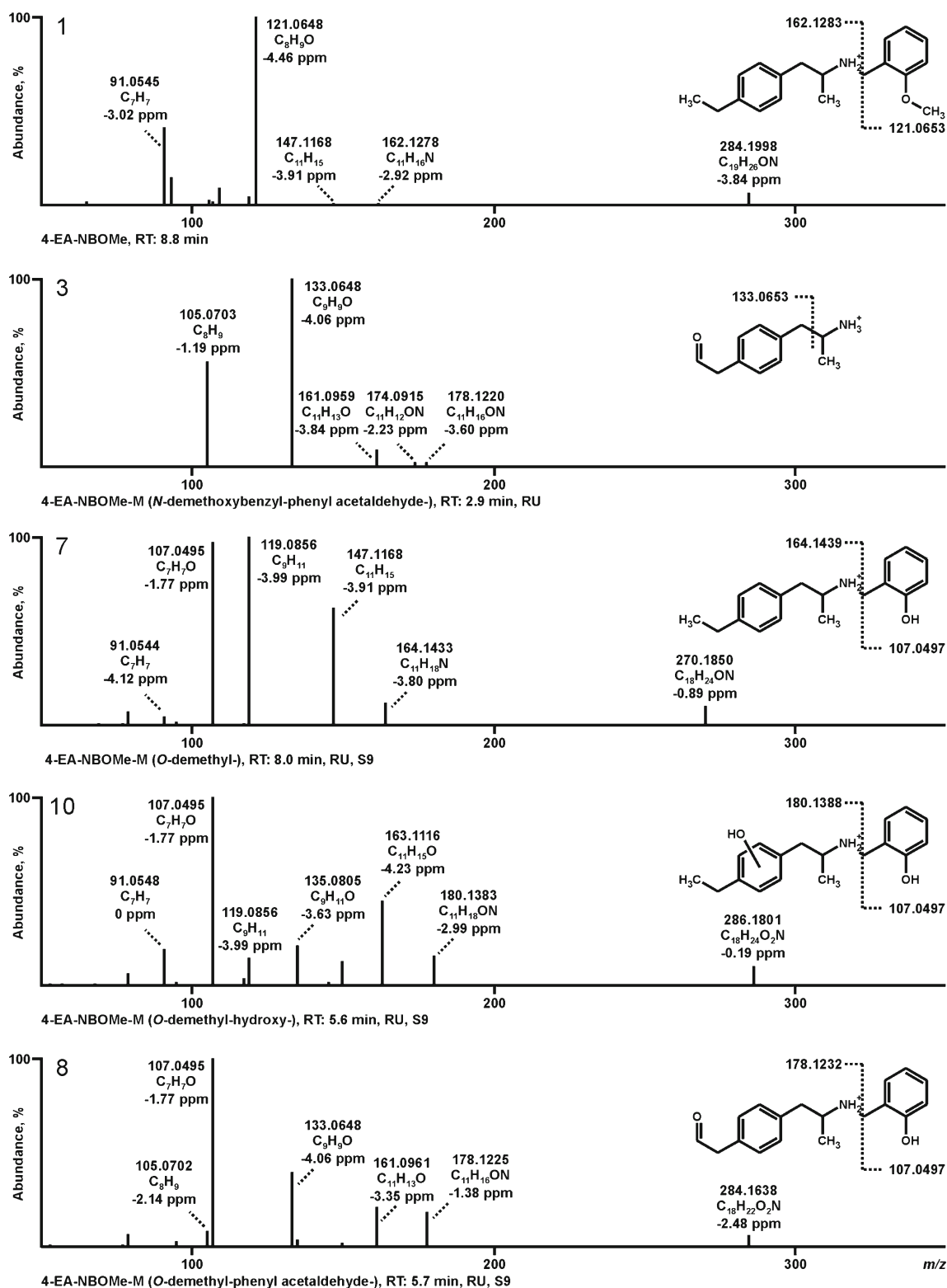
Fig. 1 HR-MS/MS spectra, proposed structures, retention times (*RT*), detected in rat urine (*RU*) and/or pooled human S9 fraction incubations (*S9*), and predominant fragmentation patterns of 4-EA-NBOMe and selected phase I metabolites arranged according to their presentation in the text

detected, so it could be assumed that the α-carbon next to the aromatic ring system should not be oxidized forming a cathinone-like structure. The third and fourth possible positions for oxidation were the two carbon atoms of the ethyl side chain. The most probable position for oxidation should be the position at the first carbon next to the aromatic ring system
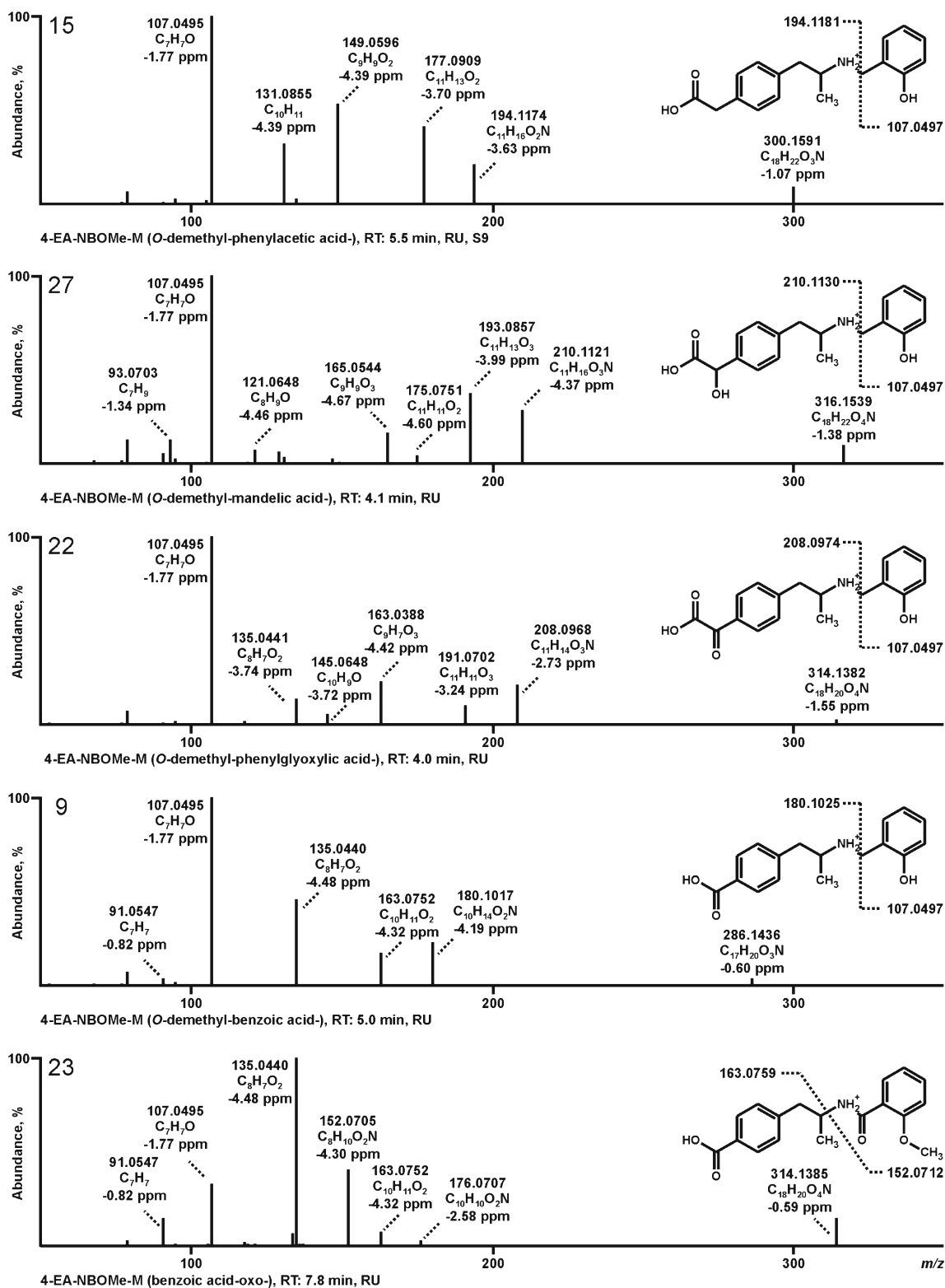
Fig. 1 (continued)

forming an acetophenone-like derivative. This metabolite was described as one of the main excretion products of ethylbenzene in rats and humans [42–44]. But concerning the MS^2 spectrum of the N-demethoxybenzyl-phenyl acetaldehyde metabolite (**3**), the assumed acetophenone derivative could not produce the fragment ion at m/z 105.0704 ($C_8H_9^+$). Of

course, an assumed N-demethoxybenzyl-acetophenone metabolite should also produce all fragment ions described above, but a loss of CO (-27.9949 u) from the fragment ion at m/z 133.0653 ($C_9H_9O^+$) to m/z 105.0704 ($C_8H_9^+$) should not be possible in an assumed acetophenone-like structure. Therefore, the suggested position for oxidation of the N-demethoxybenzyl metabolite (**2**) was the second carbon of the ethyl side chain producing a phenyl acetaldehyde-like structure. However, metabolites with an aldehyde structure usually are not stable due to fast metabolic oxidation to the corresponding carboxylic acids and/or reduction to the corresponding primary alcohols although these intermediates could often not be found. But in this case, this phenyl acetaldehyde might be stabilized by mesomeric effects. In the MS^2 spectrum of the N-demethoxybenzyl-phenyl acetaldehyde metabolite (**3**, PM at m/z 178.1226, $C_{11}H_{16}ON^+$), initial loss of four hydrogens (-4.0307, 4H) could be observed producing the fragment ion at m/z 174.0919 ($C_{11}H_{12}ON^+$). The authors assume that this loss could be caused by the free pair of electrons of the nitrogen, which could take part at the resonance stabilizing producing a completely conjugated system under the described ion source and MS conditions. However, the corresponding phenylacetic acid metabolite (**6**) could also be found and both metabolites with and without combination of other metabolic reactions.

O-Demethyl-4-EA-NBOMe

The O-demethyl metabolite (**7**, PM at m/z 270.1852, $C_{18}H_{24}ON^+$) showed characteristic fragmentation patterns. The O-demethylated NBOMe part led to the fragment ion at m/z 107.0497 ($C_7H_7O^+$). As described above, the fragment ion formed by the NBOMe part was used for identification and the fragment ions of the amphetamine core for confirmation of the suggested metabolite and its molecular formulas and structures. The fragment ion at m/z 164.1433 ($C_{11}H_{18}N^+$) represented the benzyl cleavage of O-demethyl-4-EA-NBOMe. As already described for 25I-NBOMe [5], O-demethylation of the NBOMe part produced a primary amine (m/z 164.1433, $C_{11}H_{18}N^+$) instead of an iminium ion (m/z 162.1283, $C_{11}H_{16}N^+$) as seen for the parent compound. Further breakdown of the fragment ion representing the amphetamine part was according to the described fragmentation pattern of the N-demethoxybenzylated metabolites and could be seen for most of the metabolites (with the expected shifts of the suggested metabolic reaction). A loss of ammonia (-17.0260 u, NH$_3$) formed the fragment ion at m/z 147.1174 ($C_{11}H_{15}^+$) and further loss of an ethylene group (-28.0313 u, C_2H_4) the most abundant fragment ion at m/z 119.0861 ($C_9H_{11}^+$).

O-Demethyl-hydroxy-4-EA-NBOMe

The MS^2 spectrum of the O-demethyl-hydroxy metabolite (**10**, PM at m/z 286.1802, $C_{18}H_{24}O_2N^+$) showed similar fragmentation pattern as the O-demethyl metabolite with the expected shifts of the hydroxy group ($+15.9949$ u, O). After benzyl cleavage, the fragment ions at m/z 107.0497 ($C_7H_7O^+$) and m/z 180.1388 ($C_{11}H_{18}ON^+$) were formed, followed by loss of ammonia and ethylene producing fragment ions at m/z 163.1123 ($C_{11}H_{15}O^+$) and m/z 135.0810 ($C_9H_{11}O^+$), respectively. The loss of oxygen (-15.9949 u, O) produced a fragment ion at m/z 119.0861 ($C_9H_{11}^+$). Hydroxylation at the NBOMe part would lead to a fragment ion at m/z 123.0446 ($C_7H_7O_2^+$) and no fragment ion at m/z 107.0497 ($C_7H_7O^+$) should be found. However, hydroxylation at the NBOMe part could also be observed with and without O-demethylation (**11** and **18**). Furthermore, it was expected that this metabolite could be the precursor for the oxidation to the corresponding aldehyde metabolite. Hydroxylation should take place at the ethyl side chain producing 1- and/or 2-phenylethanol, which would be in accordance to the described ethylbenzene metabolism in rats and humans [42–44]. But both 1-phenylethanol as well as 2-phenylethanol should show an initial loss of water or at least a significant loss of water from any fragment ion carrying the hydroxy group. Concerning the MS^2 spectrum of the O-demethyl-hydroxy metabolite (**10**), no significant loss of water (-18.0106 u, H$_2$O) of any fragment ion could be observed. Therefore, aromatic hydroxylation at the amphetamine core was concluded. However, only two isomers of O-demethyl-hydroxy metabolites (**10** and **11**) could be detected leading to the assumption that a possible 1-phenylethanol metabolite could not be found probably due to fast oxidation to the corresponding phenyl acetaldehyde metabolite (**8**). The exact position of the hydroxy group in the aromatic ring system could not be elucidated by the applied methods.

O-Demethyl-phenyl acetaldehyde-4-EA-NBOMe

The MS^2 spectrum of the O-demethyl-phenyl acetaldehyde metabolite (**8**, PM at m/z 284.1645, $C_{18}H_{22}O_2N^+$) showed characteristics described above for the N-demethoxybenzyl-phenyl acetaldehyde metabolite (**3**) and the O-demethyl metabolite (**7**) as well. Again, the benzyl cleavage produced the fragment ions of m/z 107.0497 ($C_7H_7O^+$) and m/z 178.1232 ($C_{11}H_{16}ON^+$), followed by loss of ammonia and ethylene, respectively. Also, a loss of CO (-27.9949 u) of the fragment ion at m/z 133.0653 ($C_9H_9O^+$) producing the fragment ion at m/z 105.0704 ($C_8H_9^+$) could be observed supporting the above suggestion of an aldehyde metabolite.

O-Demethyl-phenylacetic acid-4-EA-NBOMe

As described above, the O-demethyl-phenyl acetaldehyde metabolite could be further oxidized to the corresponding O-demethyl-phenylacetic acid metabolite (**15**, PM at m/z 300.1594, $C_{18}H_{22}O_3N^+$). This was in accordance to the described ethylbenzene metabolism in rats and humans [42–44].

The fragmentation pattern of this metabolite was similar to that of the corresponding aldehyde metabolite. Benzyl cleavage produced the characteristic NBOMe fragment ion at m/z 107.0497 ($C_7H_7O^+$) and the amphetamine core fragment ion at m/z 194.1181 ($C_{11}H_{16}O_2N^+$), followed by loss of ammonia and ethylene as already described. In addition, the fragment ion at m/z 131.0861 ($C_{10}H_{11}^+$) could be produced by a loss of CH_2O_2 (-46.0055 u) from the fragment ion at m/z 177.0916 ($C_{11}H_{13}O_2^+$) leading to the suggested phenylacetic acid metabolite.

O-Demethyl-mandelic acid-4-EA-NBOMe

According to the metabolism of ethylbenzene in rats and humans [42–44], the O-demethyl-phenylacetic acid metabolite (**15**) could be further oxidized to the O-demethyl-mandelic acid metabolite (**27**, PM at m/z 316.1543, $C_{18}H_{22}O_4N^+$). The fragmentation pattern was similar to those of the other described O-demethylated metabolites. The characteristic fragment ion at m/z 107.0497 ($C_7H_7O^+$) could also be found as the other fragment ions formed by the amphetamine part after benzyl cleavage, loss of ammonia, and loss of ethylene, respectively. In contrast to previous described fragmentation patterns [5, 6], in this MS^2 spectrum, the low-abundant fragment ion at m/z 121.0653 ($C_8H_9O^+$) should not be formed by the NBOMe part rather than by elimination of CO_2 (-43.9899 u) of the fragment ion at m/z 165.0552 ($C_9H_9O_3^+$) confirming the assumed carboxylic acid. In addition, the relative low-abundant fragment ion at m/z 175.0759 ($C_{11}H_{11}O_2^+$) could be formed by a loss of water (-18.0106 u, H_2O) from the fragment ion at m/z 193.0865 ($C_{11}H_{13}O_3^+$), which could be a hint to confirm the suggested structure of the mandelic acid. However, the exact position of the hydroxy group could not be elucidated. Aromatic hydroxylation or hydroxylation at the two carbon atoms of the phenethylamine partial structure could not completely be excluded. However, due to the described metabolism of ethylbenzene, the structure was proposed as O-demethyl-mandelic acid.

O-Demethyl-phenylglyoxylic acid-4-EA-NBOMe

Also in accordance to the metabolism of ethylbenzene, the O-demethyl-mandelic acid metabolite (**27**) could be further oxidized to the O-demethyl-phenylglyoxylic acid metabolite (**22**, PM at m/z 314.1387, $C_{18}H_{20}O_4N^+$). Again, after O-demethylation, the characteristic fragment ion at m/z 107.0497 ($C_7H_7O^+$) was found and the corresponding fragment ions of the amphetamine core after benzyl cleavage, loss of ammonia, and loss of ethylene, respectively. In addition, characteristic loss of CH_2O_2 (-46.0055 u) from the fragment ion at m/z 191.0708 ($C_{11}H_{11}O_3^+$) forming the fragment ion at m/z 145.0653 ($C_{10}H_9O^+$) and of CO (-27.9949 u) from the fragment ion at m/z 163.0395 ($C_9H_7O_3^+$) forming the fragment ion

at m/z 135.0446 ($C_8H_7O_2^+$) could be found for this metabolite. Due to these losses and according to the metabolism of ethylbenzene, the molecular structure of the metabolite was proposed as O-demethyl-phenylglyoxylic acid.

O-Demethyl-benzoic acid-4-EA-NBOMe

In the metabolism of ethylbenzene, the main excretion product in rat urine was described as benzoic acid [43, 44]. Beside oxidation to phenyl acetaldehyde and phenylacetic acid, the ethyl side chain could also be oxidized under a loss of a carbon atom to benzoic acid, here exemplified at the O-demethyl-benzoic acid metabolite (**9**, PM at m/z 286.1438, $C_{17}H_{20}O_3N^+$). The characteristic fragment ion at m/z 107.0497 ($C_7H_7O^+$) indicated O-demethylation. The fragmentation pattern of the amphetamine part was according to the O-demethyl-phenylacetic acid metabolite (**15**) with the shift of CH_2 (-14.0156 u) of all fragment ions compared to those described for the phenyl acetic acid. The expected loss of the carboxy group from the fragment ion at m/z 163.0759 ($C_{10}H_{11}O_2^+$) could not be found for the benzoic acid metabolite. However, the fragment ion at m/z 135.0446 ($C_8H_7O_2^+$) could eliminate CO_2 (-43.9899 u) producing the fragment ion at m/z 91.0548 ($C_7H_7^+$).

Benzoic acid-oxo-4-EA-NBOMe

The MS^2 spectrum of the benzoic acid-oxo metabolite (**23**, PM at m/z 314.1387, $C_{18}H_{20}O_4N^+$) showed an untypical fragmentation pattern compared to those of the previous described metabolites. Again the fragment ion at m/z 107.0497 ($C_7H_7O^+$) was present usually representing O-demethylation of the NBOMe part. The most abundant fragment ion at m/z 135.0446 ($C_8H_7O_2^+$) usually indicated benzoic acid-like structure as exemplified for the O-demethyl-benzoic acid metabolite (**9**). O-demethylation and additional oxidation of the ethyl group to benzoic acid would lead to an expected molecular formula ($C_{17}H_{20}O_3N^+$) with two carbon atoms less than the molecular formula of the parent compound ($C_{19}H_{26}ON^+$, see O-demethyl-benzoic acid metabolite, **9**). However, the suggested molecular formula was $C_{18}H_{20}O_4N^+$ so that in this case, the fragment ion at m/z 107.0497 ($C_7H_7O^+$) could not be used to identify the metabolite as O-demethyl. Nevertheless, missing the fragment ion at m/z 121.0653 ($C_8H_9O^+$) was not in accordance to previously described fragmentation properties. In addition, the fragment ion at m/z 152.0705 ($C_8H_{10}O_2N^+$) seemed to confirm the suggestion of untypical fragmentation pattern. Based on the suggested molecular formula, the relatively late retention time of 7.8 min, the pattern, and the fragment ions at m/z 152.0705 ($C_8H_{10}O_2N^+$) and m/z 176.0712 ($C_{10}H_{10}O_2N^+$), the metabolite was suggested as benzoic acid-oxo metabolite with oxidation at the carbon atom of the benzyl rest of the NBOMe part forming an amide structure. However, this position was not expected and not the most probable for oxidation because the intermediate would be a

hemiaminal and amide formation was not described yet in previous NBOMe metabolism studies [5–7, 45].

As shown in Tables S1 and S2 (see ESM), various numbers of metabolites could be detected. Besides the described identification procedure, LC-HR-MS/MS was a powerful tool for elucidating the 4-EA-NBOMe metabolism, particularly for the differentiation of metabolites with the same nominal masses in FS. For example, the nominal mass of m/z 300 could be found for at least six proposed metabolites (**13–18**). With HR-MS FS data, it could be shown that four (**13–16**, PM at m/z 300.1594, $C_{18}H_{22}O_3N^+$) of them had different accurate masses and different molecular composition within 5 ppm deviation from the calculated exact mass compared to the other two metabolites (**17** and **18**, PM at m/z 300.1958, $C_{19}H_{24}O_2N^+$). This was the case for many detected metabolites (e.g., nominal masses of m/z 314 for **22–26** or m/z 316 for **27–30**). Therefore, the combination of HR-MS FS data and HR-MS/MS spectra was a very helpful and time-saving tool for 4-EA-NBOMe metabolite identification.

LC-HR-MS for identification of the phase II metabolites based on MS/MS fragmentation

Numbering of the phase II metabolites was in accordance to the corresponding phase I metabolites (ESM Table S1) with an additional letter indicating conjugation (**G** for glucuronidation and **S** for sulfation). Fragments of the conjugates' spectra also present in those of the corresponding phase I metabolites were not discussed here. In total, 33 phase II metabolites could be identified. As shown in Table S2 (see ESM), all glucuronides eliminated dehydrated glucuronic acid (−176.0321 u) and all sulfates dehydrated sulfuric acid (−79.9568 u). For some phase II metabolites, fragment ions still containing the corresponding conjugate could help to evaluate the position of conjugation. The fragment ion at m/z 230.0487 ($C_9H_{12}O_4NS^+$) represented the O-demethylated NBOMe part conjugated with a sulfate group and could be found in the spectra of several O-demethylated and sulfated metabolites (**8S**, **9S**, **15S**, and **22S**). Also, the fragment ions at m/z 203.0014 ($C_7H_7O_5S^+$, **19S** and **31S**), m/z 217.0171 ($C_8H_9O_5S^+$, **18S** and **28S**), and m/z 246.0436 ($C_9H_{12}O_5NS^+$, **14S**) could be found as representatives for metabolites sulfated at the NBOMe part. The fragment ion at m/z 259.0640 ($C_{11}H_{15}O_5S^+$, **20S**) was identified as the sulfuric acid conjugate of the O-demethyl metabolite bis-hydroxylated at the amphetamine core (**20**). Furthermore, some fragment ions carrying the glucuronic acid could be detected. The fragment ions at m/z 299.0767 ($C_{13}H_{15}O_8^+$, **14G**), m/z 313.0923 ($C_{14}H_{17}O_8^+$, **18G** and **30G**), m/z 326.1240 ($C_{15}H_{20}O_7N^+$, **10G**), and m/z 342.1189 ($C_{15}H_{20}O_8^+$, **21G**) represented the NBOMe part conjugated with glucuronic acid. In addition, the fragment ion at m/z 356.1345 ($C_{16}H_{22}O_8N^+$, **9G₁** and **9G₂**) was identified as conjugate of glucuronic acid at the benzoic acid of the amphetamine part.

Comparison of metabolite formation in vitro after 1- and 8-h incubation and in vivo
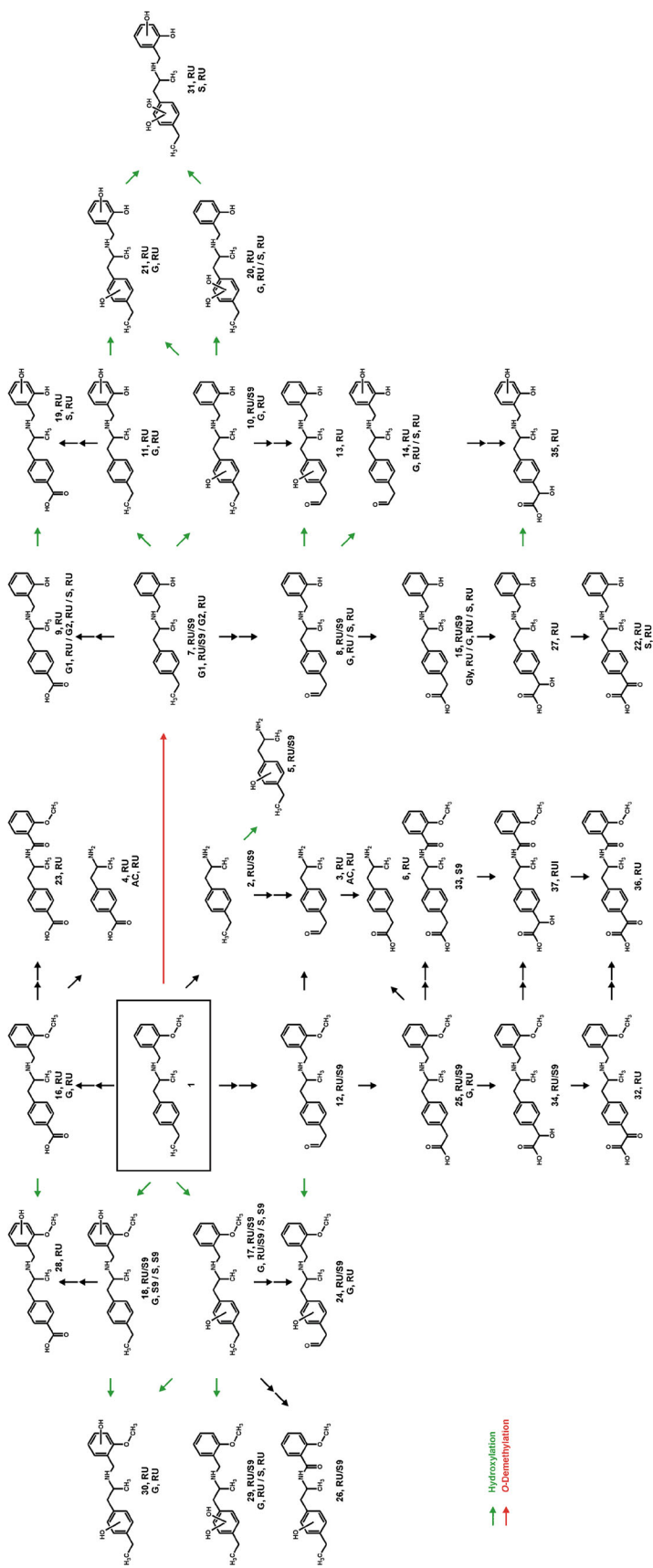
Phase I metabolites

Due to the lack of authentic human urine samples, incubations with human pS9 fraction were performed to compare the metabolites formed by rats and humans. According to Table S1 (see ESM), 35 out of 36 phase I metabolites could be detected in rat urine, 13 in pS9 after 1 h, and 15 after 8 h incubation, respectively. Fourteen metabolites could be detected in both models to confirm the metabolites, which were common for both species. The main difference between both models was the oxidation of the ethyl side chain. Metabolism studies of ethylbenzene in Wistar rats and humans [42–44] showed that benzoic acid was only described for rats. In accordance, the benzoic acid metabolite (**16**) and combinations with other metabolic reactions (**4**, **9**, **19**, **23**, and **28**) were only detected in rat urine and not in the pS9 incubations. Furthermore, the O-demethylation seemed to play a minor role in human pS9 since more O-demethylated metabolites were detected in rat urine. However, differences could also be caused by the need of multiple reaction stages to form the corresponding metabolites (e.g., O-demethyl-phenyl acetaldehyde-hydroxy, **13**). It should also be kept in mind that the rat urine was collected over 24 h, so the metabolites of the late phase of excretion were also present, which probably could not be formed in the in vitro assay. In summary, the metabolic steps such as O-demethylation, N-demethoxybenzylation, hydroxylation, and oxidation were comparable in both species except for the oxidation to benzoic acid.

Phase II metabolites

Five out of 33 phase II metabolites could be detected in pS9 incubations and 30 in rat urine (ESM Table S2). However, only two (O-demethyl and hydroxy glucuronides, **7G₁** and **17G**) were found for both models. The two hydroxy sulfates (**17S** and **18S**) and one hydroxy glucuronide (**18G**) were only detectable in the pS9 incubations. This is in accordance with a study on methamphetamine in which rats formed higher amounts of glucuronides than sulfates [46]. The low formation of phase II metabolites in pS9 incubations was already described by Richter et al. [34] and could be caused by low formation of the underlying phase I metabolites. To evaluate targets for SUSAs, a combination of both, in vitro incubations and in vivo models, should be used at least for phase II metabolites.

Proposed metabolic pathways

As shown in Fig. 2, 4-EA-NBOMe was extensively metabolized in rats as well as in human pS9. According to the metabolism of ethylbenzene in rats and humans [42–44], the

Fig. 2 Metabolic pathway of 4-EA-NBOMe studied in rat urine (*RU*) and pooled human S9 fraction incubations (*S9*). Phase II metabolites: glucuronides (*G*), sulfates (*S*), acetyl conjugates (*AC*), and glycine (*Gly*) conjugate. Numbering according to Tables S1 and S2 (see ESM)

Table 1 General involvement of monooxygenases in the formation of the given 4-EA-NBOMe metabolites, numbering in accordance to Table S1 (see ESM)

Metabolite	CYP 1A2	CYP 2A6	CYP 2B6	CYP 2C8	CYP 2C9	CYP 2C19	CYP 2D6	CYP 2E1	CYP 3A4	CYP 3A5	FMO3
N-Demethoxybenzyl (**2**)	+	n.d.	+	n.d.	n.d.	n.d.	n.d.	n.d.	+	n.d.	n.d.
O-Demethyl (**7**)	+	n.d.	+	n.d.	+	n.d.	n.d.	n.d.	+	n.d.	n.d.
Phenyl acetaldehyde (**12**)	+	n.d.	n.d.	n.d.	n.d.	+	+	n.d.	+	n.d.	n.d.
Hydroxy (**17**)	+	n.d.	+	n.d.	+	+	n.d.	n.d.	+	+	n.d.
Hydroxy-NBOMe (**18**)	+	n.d.	+	n.d.	n.d.	n.d.	n.d.	n.d.	n.d.	n.d.	n.d.

n.d. metabolite formation not detected

predominant pathway was oxidation of the ethyl side chain, e.g., to a benzoic acid derivative (**16**). This metabolite could further be *N*-demethoxybenzylated (**4**) or oxidized at the NBOMe part, forming a hydroxy metabolite (**28**) and an oxo metabolite (**23**), respectively. In addition to the oxidation to benzoic acid derivatives, the ethyl side chain could be oxidized to a phenyl acetaldehyde derivative (**12**) with further oxidation to a phenylacetic acid derivative (**25**). Both could additionally be *N*-demethoxybenzylated (**3** and **6**) or further oxidized to the phenyl acetaldehyde-hydroxy (**24**) or the phenylacetic acid-oxo derivatives (**33**). However, the intermediates of the oxidations (1- and/or 2-phenylethanol, marked as double arrows in Fig. 2) could not be found probably due to low stability or fast oxidation. According to the metabolism to ethylbenzene [42–44], both phenylacetic acid derivatives (**25** and **33**) could further be oxidized to the corresponding mandelic acid (**34**) and phenylglyoxylic acid (**32**) derivatives. Oxidation at the NBOMe part formed the mandelic acid-oxo (**37**) and phenylglyoxylic acid-oxo derivatives (**36**), respectively. Hydroxylation of the parent compound could occur at both, the amphetamine core (**17**) and the NBOMe part (**18**), followed by second hydroxylation forming two isomers of *bis*-hydroxylated metabolite (**29** and **30**) as well as by further oxidation to an oxo-hydroxy metabolite (**26**). All described pathways (left part in Fig. 2) could also be found after *O*-demethylation (**7**) of 4-EA-NBOMe (right part in Fig. 2). *O*-Demethylation in combination with hydroxylations at both parts (**10** and **11**) followed by second hydroxylation (**20** and **21**) and additionally by third hydroxylation (**31**) could also be observed. Furthermore, *O*-demethylation in combination with oxidation to phenyl acetaldehyde (**8**), benzoic acid (**9**), or phenylacetic acid derivatives (**15**) as well as further oxidation to mandelic acid (**27**) and phenylglyoxylic acid derivatives (**22**) could be found. As described for 4-EA-NBOMe without *O*-demethylation, these metabolites could occur in combination with hydroxylation at the amphetamine core (**13**) or at the NBOMe part (**14**, **19**, and **35**). Compared to the pathways without *O*-demethylation, it should be mentioned that oxo metabolites (amide structure, **23**, **26**, **33**, **36**, and **37**) in combination with *O*-demethylation could not be found. This could be caused by a suggested hydrogen bond between the secondary

amine and the resulting hydroxy group after *O*-demethylation [5], which could lead to a steric hindrance for amide formation at the NBOMe part. *N*-Demethoxybenzylation forming 4-EA (**2**) seemed to play a minor role in the metabolism of 4-EA-NBOMe. However, some metabolites could be detected either after *N*-demethoxybenzylation of the corresponding 4-EA-NBOMe metabolite (**12**, **16**, **17**, or **25**) or after further oxidation of 4-EA leading to phenyl acetaldehyde (**3**), benzoic acid (**4**), phenylacetic acid (**6**), or hydroxy (**5**) derivatives.

The main phase I metabolites were conjugated with glucuronic acid or sulfuric acid. The most conjugated metabolites could be found after initial *O*-demethylation according to Fig. 2. Glucuronidation (G) or sulfation (S) could be found for both hydroxy isomers (**17G/S** and **18G/S**), for both *bis*-hydroxy isomers (**29G/S** and **30G**) as well as for the *O*-demethyl-phenyl acetaldehyde derivative (**8G/S**) and in combination with hydroxylation at the NBOMe part (**14G/S**), for the *O*-demethyl-benzoic acid derivative (**9G$_1$**, **9G$_2$**, and **9S**), and for the *O*-demethyl-phenylacetic acid derivative (**15G/S**). Only glucuronidation could be found for the benzoic acid derivative (**16G**), the phenyl acetic acid derivative (**25G**), as well as for the *O*-demethyl metabolite (**7G$_1$** and **7G$_2$**), for both *O*-demethyl-hydroxy metabolites (**10G** and **11G**) and for both *O*-demethyl-*bis*-hydroxy isomers (**20G** and **21G**). As described above, for the *O*-demethyl metabolite (**7G$_1$** and **7G$_2$**) and the *O*-demethyl-benzoic acid derivative (**9G$_1$** and **9G$_2$**), two isomers with similar MS^2 spectra could be detected and separated on the used chromatographic system. Caused by the enantioselective conjugation with glucuronic acid, two diastereomers could be possible after administration or incubations with racemic 4-EA-NBOMe, respectively.

Only sulfation could be found for the *O*-demethyl-benzoic acid-hydroxy-NBOMe derivative (**19S**), the *O*-demethyl-phenylglyoxylic acid (**22S**), and the *O*-demethyl-*bis*-hydroxy-hydroxy-NBOMe derivatives (**31S**). Furthermore, *N*-acetylation (AC) could be found for the phenyl acetaldehyde (**3AC**) and the benzoic acid (**4AC**) derivatives after *N*-demethoxybenzylation. In addition and in accordance to the metabolism of ethylbenzene in rats [43], the *O*-demethyl-phenylacetic acid derivative could also be conjugated with glycine (**15Gly**). Glycine conjugates of other oxidation

Table 2 Detected 4-EA-NBOMe metabolites, molecular mass, five relevant EI-GC-MS fragment ions, and retention indices (RI), in rat urine after low dosages by GC-MS SUSA

No.	Target for SUSA	Molecular mass, u	GC-MS fragment ions, m/z and their relative intensities, %	RI
16	4-EA-NBOMe-M (benzoic acid-) MEAC	355	91 (63), 121 (100), 164 (19), 206 (55), 355 (2)	2770
17	4-EA-NBOMe-M (hydroxy-) 2AC	383	91 (44), 121 (100), 206 (40), 250 (6), 383 (1)	2870
29	4-EA-NBOMe-M (*bis*-hydroxy-) 3AC	441	91 (67), 121 (100), 206 (90), 250 (7), 441 (4)	3020

The numbers correspond to those of ESM Table S1

AC acetylation after derivatization, *ME* artificial methylation

products of the ethyl side chain could not be found (e.g., conjugation of benzoic acid forming hippuric acid [43]).

Monooxygenase activity screening

For identification of the monooxygenases catalyzing the initial metabolic steps, first, the ten most abundant human hepatic CYPs were incubated under conditions allowing a statement on the general involvement of a particular enzyme. It should be kept in mind that these qualitative data did not reflect a quantitative contribution of the investigated monooxygenases to the hepatic clearance that would require the collection of enzyme kinetic data [47], which was beyond the scope of this study. As summarized in Table 1, CYP1A2, CYP2B6, and CYP3A4 were involved in almost every initial metabolic step like *N*-demethoxybenzylation, *O*-demethylation, or hydroxylation at both parts of the compound. Hydroxylation at the NBOMe part was only catalyzed by CYP1A2 and CYP2B6.

In addition, the contribution of FMO3 as the relevant flavin-containing monooxygenase involved in the metabolism of several NPS [36] was elucidated, but no involvement in the 4-EA-NBOMe metabolism could be detected.

Toxicological detection of 4-EA-NBOMe by SUSAs

In accordance with other compounds of the NBOMe class [5–7], the parent compound was not or only in traces detectable in urine and should not be used as target for urine screening procedures. The most abundant metabolites in the high-dose (10 mg/kg BW) rat urine samples after precipitation were the benzoic acid (**16**) and *O*-demethyl-benzoic acid (**9**) metabolites. But both were not suitable as targets for screening procedures for human consumption since oxidation to benzoic acid was not found in this study after in vitro incubations and was not described in the literature for humans. Therefore, other metabolites should be used as targets. In the

Table 3 Detected 4-EA-NBOMe metabolites, protonated precursor ions, characteristic MS^2 and MS^3 fragment ions, and retention times (RT), in rat urine after low dosages by LC-MS^n SUSA

No.	Target for SUSA	Precursor ions, m/z	MS^2 fragment ions, m/z and relative intensity, %	MS^3 fragment ions, m/z, and relative intensity, in %, on the ion given in bold	RT, min
9	4-EA-NBOMe-M (*O*-demethyl-benzoic acid-)	286	107 (9), 135 (8), 163 (18), 180 (100)	**163:** 91 (3), 105 (1), 135 (100) **180:** 91 (2), 105 (1), 135 (100)	7.2
15	4-EA-NBOMe-M (*O*-demethyl-phenylacetic acid-)	300	107 (2), 121 (7), 149 (8), 177 (49), 194 (100)	**177:** 131 (23), 149 (100) **194:** 131 (25), 149 (100)	8.2
16	4-EA-NBOMe-M (benzoic acid-)	300	91 (12), 93 (6), 121 (100)	**121:** 91 (23), 93 (100)	8.9
20	4-EA-NBOMe-M (*O*-demethyl-*bis*-hydroxy-)	302	107 (4), 150 (11), 179 (66), 196 (100)	**179:** 91 (9), 117 (10), 133 (9), 143 (26), 151 (100) **196:** 91 (9), 117 (11), 133 (10), 143 (27), 151 (100)	5.8
25	4-EA-NBOMe-M (phenylacetic acid-)	314	91 (14), 93 (5), 121 (100), 192 (9), 251 (5)	**121:** 91 (23), 93 (100)	9.8
27	4-EA-NBOMe-M (*O*-demethyl-mandelic acid-)	316	107 (2), 165 (3), 193 (43), 210 (100)	**193:** 107 (12), 121 (15), 147 (10), 165 (100) **210:** 107 (9), 121 (12), 149 (11), 165 (100), 175 (22)	5.5
32	4-EA-NBOMe-M (phenylglyoxylic acid-)	328	93 (1), 121 (100), 284 (2)	**121:** 91 (23), 93 (100) **284:** 91 (13), 93 (11), 121 (100)	6.4
34	4-EA-NBOMe-M (mandelic acid-)	330	93 (1), 121 (100), 208 (6)	**121:** 91 (23), 93 (100) **208:** 107 (1), 131 (7), 149 (100), 162 (5)	6.7
16G	4-EA-NBOMe-M (benzoic acid-) glucuronide	476	135 (1), 180 (7), 300 (100)	**180:** 91 (2), 105 (1), 135 (100) **300:** 91 (12), 93 (6), 121 (100)	6.7
17G	4-EA-NBOMe-M (hydroxy-) glucuronide	476	178 (1), 300 (100)	**178:** 119 (100) **300:** 91 (10), 93 (4), 119 (1), 121 (100)	8.1
29G	4-EA-NBOMe-M (*bis*-hydroxy-) glucuronide	492	178 (1), 313 (3), 316 (100)	**313:** 107 (10), 137 (100) **316:** 91 (10), 93 (6), 121 (100), 194 (5)	6.2

The numbers correspond to those of Tables S1 and S2 (see ESM)

Table 4 Detected 4-EA-NBOMe metabolites, calculated masses of their precursor ions, and retention times (RT) in rat urine after low dosages by LC-HR-MS/MS SUSA

No.	Targets in SUSA	Calculated exact masses of precursor ions, *m/z*	RT, min	Rat urine 0.1 mg/kg BW
9	4-EA-NBOMe-M (*O*-demethyl-benzoic acid-)	286.1438	4.7	I
15	4-EA-NBOMe-M (*O*-demethyl-phenylacetic acid-)	300.1594	4.9	D
16	4-EA-NBOMe-M (benzoic acid-)	300.1594	5.2	I
22	4-EA-NBOMe-M (*O*-demethyl-phenylglyoxylic acid-)	314.1387	4.2	D
23	4-EA-NBOMe-M (benzoic acid-oxo-)	314.1387	6.5	I
25	4-EA-NBOMe-M (phenylacetic acid-)	314.1751	5.5	I
27	4-EA-NBOMe-M (*O*-demethyl-mandelic acid-)	316.1543	4.3	I
32	4-EA-NBOMe-M (phenylglyoxylic acid-)	328.1543	4.5	I
34	4-EA-NBOMe-M (mandelic acid-)	330.1700	4.6	I
36	4-EA-NBOMe-M (phenylglyoxylic acid-oxo-)	342.1336	5.8	D
9S	4-EA-NBOMe-M (*O*-demethyl-benzoic acid-) sulfate	366.1006	5.0	D
19S	4-EA-NBOMe-M (*O*-demethyl-benzoic acid-hydroxy-NBOMe-) sulfate	382.0955	4.5	D
16G	4-EA-NBOMe-M (benzoic acid-) glucuronide	476.1915	4.7	D
17G	4-EA-NBOMe-M (hydroxy-) glucuronide	476.2279	5.0	I
29G	4-EA-NBOMe-M (*bis*-hydroxy-) glucuronide	492.2228	4.4	D

The numbers correspond to those of Tables S1 and S2 in the ESM

D detection of the precursor ion in MS[1], *I* identification via MS[1] and MS[2]

Fig. 3 Reconstructed ion chromatograms indicating the ten most abundant metabolites in pooled human S9 fraction incubations (*S9*) and in rat urine (*RU*) after 0.1 mg/kg body weight administration by LC-HR-MS/MS standard urine screening approach. Numbering according to Table 4
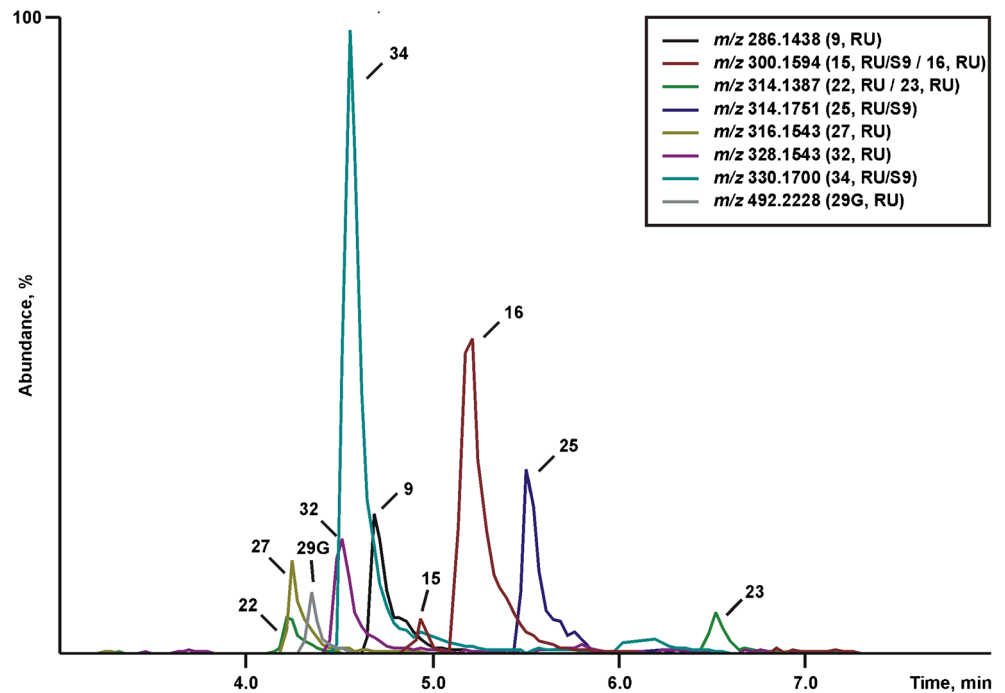
following part, the detected metabolites with the corresponding screening procedure will be discussed.

GC-MS SUSA

In contrast to previous published NBOMe studies [5, 6], an intake of 4-EA-NBOMe was detectable in the rat urine via metabolites after low-dose administration by GC-MS. A list of all detected metabolites is given in Table 2. In general, it is hard to say if an intake of 4-EA-NBOMe and/or metabolites could also be detected in authentic human urine samples due to the lack of such samples. Furthermore, the time between administration and urine sampling plays an important role for this suggestion. However, detection might be possible after at least high-dose administration in context of an acute intoxication as well as after low-dose administration in context of recreational use concerning the selected low dosage corresponding to common users' doses. However, the main targets after acidic hydrolysis and derivatization with acetic anhydride should be the hydroxy metabolite (**17**) and the *bis*-hydroxy metabolite (**29**).

LC-MS^n SUSA

The LC-MS^n approach was able to detect an intake of 4-EA-NBOMe after the 0.1-mg/kg BW dosage in rat urine. A list of the detected metabolites is given in Table 3. Again, detection of an intake of 4-EA-NBOMe should also be possible in authentic human urine samples as already described for the GC-MS SUSA. Suitable targets were the phenylacetic acid (**15** and **25**) and mandelic acid (**27** and **34**) derivatives with and without additional *O*-demethylation.

LC-HR-MS/MS SUSA

As expected, the LC-HR-MS/MS SUSA allowed the detection of 4-EA-NBOMe metabolites in the low-dose samples. A list of all detected metabolites is given in Table 4. Again, detection of an intake of 4-EA-NBOMe should also be possible in authentic human urine samples as already described for the GC-MS and LC-MS^n SUSAs. Phase I and II metabolites were suitable targets with and without conjugate cleavage. As shown in the reconstructed ion chromatograms in Fig. 3 with the ten most abundant metabolites in rat urine after 0.1 mg/kg BW administration, suggested targets were the phenylacetic acid (**15** and **25**) and the mandelic acid (**27** and **34**) derivatives with and without additional *O*-demethylation.

Conclusions

LC-HR-MS/MS was a powerful tool for elucidating the 4-EA-NBOMe metabolism, particularly for the differentiation of metabolites with the same nominal masses (e.g. *m/z* 300 for **13–18**). 4-EA-NBOMe was extensively metabolized mainly via oxidation of the ethyl side chain, *O*-demethylation, and combinations of the described metabolic reactions followed by conjugation. They consist of those described for other NBOMes and for ethylbenzene. Species differences could be found for the oxidation of the side chain to benzoic acid which could only be found in rat urine. Furthermore, mainly CYP1A2, CYP2B6, and CYP3A4 catalyzed the main metabolic reactions. An intake of 4-EA-NBOMe was detectable by all investigated SUSAs only via several phase I and II metabolites after an assumed user's dose of 0.1 mg/kg BW.

References

1. European Monitoring Centre for Drugs and Drug Addiction (EMCDDA) (2015) New psychoactive substances in Europe. An update from the EU Early Warning System. http://www.emcdda. europa.eu/attachements.cfm/att_235958_EN_TD0415135ENN.pdf

2. United Nations Office on Drugs and Crime (UNODC) (2014) World drug report 2014. http://www.unodc.org/documents/data-and-analysis/WDR2014/World_Drug_Report_2014_web.pdf

3. United Nations Office on Drugs and Crime (UNODC) (2015) World drug report 2015. https://www.unodc.org/documents/wdr2015/World_Drug_Report_2015.pdf

4. United Nations Office on Drugs and Crime (UNODC) (2016) World drug report 2016. https://www.unodc.org/doc/wdr2016/WORLD_DRUG_REPORT_2016_web.pdf

5. Caspar AT, Helfer AG, Michely JA, Auwaerter V, Brandt SD, Meyer MR, et al. Studies on the metabolism and toxicological detection of the new psychoactive designer drug 2-(4-iodo-2,5-dimethoxyphenyl)-N-[(2-methoxyphenyl)methyl]ethanamine (25I-NBOMe) in human and rat urine using GC-MS, LC-MSn, and LC-HR-MS/MS. Anal Bioanal Chem. 2015;407:6697–719.

6. Caspar AT, Brandt SD, Stoever AE, Meyer MR, Maurer HH. Metabolic fate and detectability of the new psychoactive substances 2-(4-bromo-2,5-dimethoxyphenyl)-N-[(2-methoxyphenyl)methyl]ethanamine (25B-NBOMe) and 2-(4-chloro-2, 5-dimethoxyphenyl)-N-[(2-methoxyphenyl)methyl]ethanamine (25C-NBOMe) in human and rat urine by GC-MS, LC-MS^n, and LC-HR-MS/MS approaches. J Pharm Biomed Anal. 2017;134:158–69.

7. Wohlfarth A, Roman M, Andersson M, Kugelberg FC, Diao X, Carlier J, et al. 25C-NBOMe and 25I-NBOMe metabolite studies

in human hepatocytes, in vivo mouse and human urine with high-resolution mass spectrometry. Drug Test Anal. 2017;9:680–98.

8. Suzuki J, Dekker MA, Valenti ES, Arbelo Cruz FA, Correa AM, Poklis JL, et al. Toxicities associated with NBOMe ingestion—a novel class of potent hallucinogens: a review of the literature. Psychosomatics. 2015;56:129–39.

9. Zuba D, Sekula K, Buczek A. 25C-NBOMe—new potent hallucinogenic substance identified on the drug market. Forensic Sci Int. 2013;227:7–14.

10. Poklis JL, Charles J, Wolf CE, Poklis A. High-performance liquid chromatography tandem mass spectrometry method for the determination of 2CC-NBOMe and 25I-NBOMe in human serum. Biomed Chromatogr. 2013;27:1794–800.

11. Poklis JL, Clay DJ, Poklis A. High-performance liquid chromatography with tandem mass spectrometry for the determination of nine hallucinogenic 25-NBOMe designer drugs in urine specimens. J Anal Toxicol. 2014;38:113–21.

12. Poklis JL, Nanco CR, Troendle MM, Wolf CE, Poklis A. Determination of 4-bromo-2,5-dimethoxy-N-[(2-methoxyphenyl)methyl]-benzeneethanamine (25B-NBOMe) in serum and urine by high performance liquid chromatography with tandem mass spectrometry in a case of severe intoxication. Drug Test Anal. 2014;6:764–9.

13. Poklis JL, Devers KG, Arbefeville EF, Pearson JM, Houston E, Poklis A. Postmortem detection of 25I-NBOMe [2-(4-iodo-2,5-dimethoxyphenyl)-N-[(2-methoxyphenyl)methyl]ethanamine] in fluids and tissues determined by high performance liquid chromatography with tandem mass spectrometry from a traumatic death. Forensic Sci Int. 2014;234:e14–20.

14. Poklis JL, Raso SA, Alford KN, Poklis A, Peace MR. Analysis of 25I-NBOMe, 25B-NBOMe, 25C-NBOMe and other dimethoxyphenyl-N-[(2-methoxyphenyl) methyl]ethanamine derivatives on blotter paper. J Anal Toxicol. 2015;39:617–23.

15. Boumrah Y, Humbert L, Phanithavong M, Khimeche K, Dahmani A, Allorge D. In vitro characterization of potential CYP- and UGT-derived metabolites of the psychoactive drug 25B-NBOMe using LC-high resolution MS. Drug Test Anal. 2016;8:248–56.

16. Nielsen LM, Holm NB, Leth-Petersen S, Kristensen JL, Olsen L, Linnet K. Characterization of the hepatic cytochrome P450 enzymes involved in the metabolism of 25I-NBOMe and 25I-NBOH. Drug Test Anal. 2017;9:671–9.

17. Temporal KH, Scott KS, Mohr ALA, Logan BK. Metabolic profile determination of NBOMe compounds using human liver microsomes and comparison with findings in authentic human blood and urine. J Anal Toxicol DOI. 2017; doi:10.1093/jat/bkx029.

18. Hill SL, Doris T, Gurung S, Katebe S, Lomas A, Dunn M, et al. Severe clinical toxicity associated with analytically confirmed recreational use of 25I-NBOMe: case series. Clin Toxicol (Phila). 2013;51:487–92.

19. Stellpflug SJ, Kealey SE, Hegarty CB, Janis GC. 2-(4-Iodo-2,5-dimethoxyphenyl)-N-[(2-methoxyphenyl)methyl]ethanamine (25I-NBOMe): clinical case with unique confirmatory testing. J Med Toxicol. 2014;10:45–50.

20. Tang MH, Ching CK, Tsui MS, Chu FK, Mak TW. Two cases of severe intoxication associated with analytically confirmed use of the novel psychoactive substances 25B-NBOMe and 25C-NBOMe. Clin Toxicol (Phila). 2014;52:561–5.

21. Walterscheid JP, Phillips GT, Lopez AE, Gonsoulin ML, Chen HH, Sanchez LA. Pathological findings in 2 cases of fatal 25I-NBOMe toxicity. Am J Forensic Med Pathol. 2014;35:20–5.

22. Suzuki J, Poklis JL, Poklis A. "My friend said it was good LSD": a suicide attempt following analytically confirmed 25I-NBOMe ingestion. J Psychoactive Drugs. 2014;46:379–82.

23. Shanks KG, Sozio T, Behonick GS. Fatal intoxications with 25B-NBOMe and 25I-NBOMe in Indiana during 2014. J Anal Toxicol. 2015;39:602–6.

24. Westphal F, Girreser U, Waldmuller D. Analytical characterization of four new ortho-methoxybenzylated amphetamine-type designer drugs. Drug Test Anal. 2016;8:910–9.

25. Braden MR, Parrish JC, Naylor JC, Nichols DE. Molecular interaction of serotonin 5-HT2A receptor residues Phe339(6.51) and Phe340(6.52) with superpotent N-benzyl phenethylamine agonists. Mol Pharmacol. 2006;70:1956–64.

26. Hansen M, Phonekeo K, Paine JS, Leth-Petersen S, Begtrup M, Brauner-Osborne H, et al. Synthesis and structure-activity relationships of N-benzyl phenethylamines as 5-HT2A/2C agonists. ACS Chem Neurosci. 2014;5:243–9.

27. Halberstadt AL, Geyer MA. Effects of the hallucinogen 2,5-dimethoxy-4-iodophenethylamine (2C-I) and superpotent N-benzyl derivatives on the head twitch response. Neuropharmacology. 2014;77:200–7.

28. Nichols DE, Sassano MF, Halberstadt AL, Klein LM, Brandt SD, Elliott SP, et al. N-benzyl-5-methoxytryptamines as potent serotonin 5-HT2 receptor family agonists and comparison with a series of phenethylamine analogues. ACS Chem Neurosci. 2015;6:1165–75.

29. Maurer HH. Chemistry, pharmacology, and metabolism of emerging drugs of abuse [review]. Ther Drug Monit. 2010;32:544–9.

30. Lawn W, Barratt M, Williams M, Horne A, Winstock A. The NBOMe hallucinogenic drug series: patterns of use, characteristics of users and self-reported effects in a large international sample. J Psychopharmacol. 2014;28:780–8.

31. Bersani FS, Corazza O, Albano G, Valeriani G, Santacroce R, Bolzan Mariotti PF, Cinosi E, Simonato P, Martinotti G, Bersani G, Schifano F (2014) 25C-NBOMe: preliminary data on pharmacology, psychoactive effects, and toxicity of a new potent and dangerous hallucinogenic drug. Biomed Res Int 734749.

32. Michely JA, Helfer AG, Brandt SD, Meyer MR, Maurer HH. Metabolism of the new psychoactive substances N,N-diallyltryptamine (DALT) and 5-methoxy-DALT and their detectability in urine by GC-MS, LC-MSn, and LC-HR-MS/MS. Anal Bioanal Chem. 2015;407:7831–42.

33. Wissenbach DK, Meyer MR, Remane D, Philipp AA, Weber AA, Maurer HH. Drugs of abuse screening in urine as part of a metabolite-based LC-MS(n) screening concept. Anal Bioanal Chem. 2011;400:3481–9.

34. Richter LHR, Flockerzi V, Maurer HH, Meyer MR. Pooled human liver preparations, HepaRG, or HepG2 cell lines for metabolism studies of new psychoactive substances? A study using MDMA, MDBD, butylone, MDPPP, MDPV, MDPB, 5-MAPB, and 5-API as examples. J Pharm Biomed Anal. 2017;143:32–42.

35. Welter J, Meyer MR, Wolf E, Weinmann W, Kavanagh P, Maurer HH. 2-Methiopropamine, a thiophene analogue of methamphetamine: studies on its metabolism and detectability in the rat and human using GC-MS and LC-(HR)-MS techniques. Anal Bioanal Chem. 2013;405:3125–35.

36. Wagmann L, Meyer MR, Maurer HH. What is the contribution of human FMO3 in the N-oxygenation of selected therapeutic drugs and drugs of abuse? Toxicol Lett. 2016;258:55–70.

37. Meyer MR, Lindauer C, Welter J, Maurer HH. Dimethocaine, a synthetic cocaine derivative: studies on its in vivo metabolism and its detectability in urine by LC-HR-MSn and GC-MS using a rat model. Anal Bioanal Chem. 2014;406:1845–54.

38. Maurer HH, Pfleger K, Weber AA. Mass spectral data of drugs, poisons, pesticides, pollutants and their metabolites. Weinheim: Wiley-VCH; 2016.

39. Helfer AG, Michely JA, Weber AA, Meyer MR, Maurer HH. Orbitrap technology for comprehensive metabolite-based liquid chromatographic-high resolution-tandem mass spectrometric urine drug screening—exemplified for cardiovascular drugs. Anal Chim Acta. 2015;891:221–33.

40. Maurer HH, Wissenbach DK, Weber AA. Maurer/Wissenbach/Weber MWW LC-MSn library of drugs, poisons, and their metabolites. Weinheim: Wiley-VCH; 2014.

41. Maurer HH, Meyer MR, Helfer AG, Weber AA. Maurer/Meyer/Helfer/Weber MMHW LC-HR-MS/MS library of drugs, poisons, and their metabolites. Weinheim: Wiley-VCH; 2017.

42. Engstrom K, Riihimaki V, Laine A. Urinary disposition of ethylbenzene and m-xylene in man following separate and combined exposure. Int Arch Occup Environ Health. 1984;54:355–63.

43. Engstrom K, Elovaara E, Aitio A. Metabolism of ethylbenzene in the rat during long-term intermittent inhalation exposure. Xenobiotica. 1985;15:281–6.

44. Saghir SA, Rick DL, McClymont EL, Zhang F, Bartels MJ, Bus JS. Mechanism of ethylbenzene-induced mouse-specific lung tumor: metabolism of ethylbenzene by rat, mouse, and human liver and lung microsomes. Toxicol Sci. 2009;107:352–66.

45. Leth-Petersen S, Gabel-Jensen C, Gillings N, Lehel S, Hansen HD, Knudsen GM, et al. Metabolic fate of hallucinogenic NBOMes. Chem Res Toxicol. 2016;29:96–100.

46. Shima N, Kamata HT, Katagi M, Tsuchihashi H. Urinary excretion of the main metabolites of methamphetamine, including p-hydroxymethamphetamine-sulfate and p-hydroxymethamphetamine-glucuronide, in humans and rats. Xenobiotica. 2006;36:259–67.

47. Wink CSD, Meyer GMJ, Meyer MR, Maurer HH. Toxicokinetics of lefetamine and derived diphenylethylamine designer drugs—contribution of human cytochrome P450 isozymes to their main phase I metabolic steps. Toxicol Lett. 2015;238:39–44.